JOURNAL OF THE SOUTHEASTERN ASSOCIATION FOR RESEARCH IN ASTRONOMY, **2**, 71-78, 2008 MAY 1

Hα STUDY OF β LYRAE

SHARON K. GRAY[1] AND RICHARD IGNACE
Department of Physics, Astronomy, and Geology
East Tennessee State University
Johnson City, TN 37614

ABSTRACT

The eclipsing binary β Lyrae has been extensively researched for more than two centuries. Spectral analysis is one method that is used to gain knowledge of its unique structure. The Hα emission has been associated with a bipolar flow component in the system. We extracted and analyzed Hα data obtained at the Ritter Observatory. The 162 Hα emission line spectra are double-peaked in appearance. We measure the equivalent width, characterize the line widths, and infer total line fluxes. We find that the line flux of Hα varies little with the orbital period of 12.9 days.

Subject headings: Stars: individual (β Lyrae, Hα) — Stars: binaries: eclipsing

1. INTRODUCTION

Located at a distance of 270 parsecs, β Lyrae is the prototype for a close eclipsing variable binary star system. The β Lyrae system has evolved nonconservatively during its 32 million year lifetime (DeGreve & Linnell, 1994). The two stars of this binary are in a circular orbit with a separation of 55-60$R_\odot$. The orbital period is approximately 12.9 days, but the period is slowly increasing at a rate of 19 seconds per year. The high rate of mass transfer between the two stars ($\approx 10^{-5} M_\odot$/year) creates a rare geometry for the system. The mass losing star, a B8 giant, fills its Roche lobe and is experiencing rapid mass transfer to the other star via a gas stream. The gainer star is completely obscured by a geometrically and optically thick circumstellar disk, but it is thought to be an early main sequence B star. The gas stream interacts with the disk, producing jet-like structures that are perpendicular to the orbital plane. A circumbinary envelope adds another element of complexity to this system. Table 1 lists the properties of the individual stars that comprise β Lyrae.

Until recently, the close proximity of these two stars (less than the distance between our sun and Mercury) prohibited resolution of the individual stars and other components of the system. Spectral analysis and other methods are used to model β Lyrae. The jet-like structures were found by Harmanec et al. (1996) using interferometry and by Hoffman et al. (1998) using ultraviolet and visual spectropolarimetry. An attempt by Linnell et al. (1998) to model β Lyrae predicts a hot electron scattering region above and below the disk of the gainer star. The jet-like structure is relevant to this study because most of the Hα emission apparently originates from this component (Harmanec et al. 1996).

The following section describes the data that were used for this study, then in §3 we analyze the spectra relative to phase, and a discussion of the results is presented in §4.

2. OBSERVATIONS

We used 169 CCD spectra of β Lyrae obtained at the Ritter Observatory (astro1.panet.utoledo.edu/~wwwphys/ritter/ritter.html) between 1993 and 2000 using their echelle spectrograph (at $R_{\max} = \lambda/\Delta\lambda = 60,000$) on their 1 m telescope. Data were obtained by various observers at the University of Toledo during this period, and reduced data were made available to use by Dr K. Bjorkman. Our analysis is based on 162 spectra that were acquired between 1996 and 2000. Seven spectra were omitted from this study because they were not used in our analysis for the following reasons: two were mispointings, two lacked identifying information, and three files were unreadable. Table 1 shows when the observations occurred. Usually, a single spectrum was obtained each night. However, multiple spectra (2-6) were acquired in rapid succession on eight nights in 1997, twice in 1998, and once in 2000.

The data are stored in fits files that are stacked in nine echelle orders between the 5285 - 6595 Å wavelengths (see Figure 1). This project involved isolating the Hα (6563 Å) line which is located in the ninth order. IDL routines were used to extract the Hα data for each of the 162 spectra (see Figure 2).

3. DATA ANALYSIS

The continuum was normalized for each spectrum. The time of each observation was converted to heliocentric Julian date. The phase of each observation was calculated using the quadratic ephemeris equation of Harmanec & Scholz (1993):

$$T = T_0 + T_1 E + T_2 E^2 \quad (1)$$

where T_0 =*HJD*2408247.966 is an arbitrary number, T_1 = $12.^{\rm d}913780$ represents the binary period at T_0, and T_2 = 3.87196×10^{-6} days represents the period change.

The continuum normalized data files were plotted to phase. The sequence of graphs in Figure 3 exemplifies how the Hα line profile changes with phase. These examples show approximately quarter phase intervals as the component stars complete one orbit. The first graph in the sequence reflects the line profile at primary eclipse when the gainer star (embedded in its accretion disk) occults the loser star. As the orbit progresses, at quarter phase, both stars become visible to the observer. The third graph shows the line profile near secondary eclipse when the loser star occults the gainer star and its disk. The fourth graph is representative of the line profile when the stars have completed three fourths of an orbit and both stars become visible to the observer.

The equivalent widths of the Hα emission lines were determined using the equation:

[1] Southeastern Association for Research in Astronomy (SARA) NSF-REU Summer Intern
Electronic address: graysk13@gmail.com; ignace@etsu.edu

TABLE 1
PROPERTIES OF THE COMPONENT STARS

Component	Gainer	Loser
Spectral Type	≈B0 V	≈B6-8 IIp
Radius	$\approx 6R_\odot$	$\approx 15R_\odot$
Mass	$\approx 13M_\odot$	$\approx 3M_\odot$
Temperature	32,000 K	13,300 K

TABLE 2
OBSERVATION DATES

Year	Months	Number of Spectra
1996	Aug.	2
1997	Apr.-Nov.	74
1998	Apr.-Oct.	29
1999	June-Sept.	41
2000	Aug.-Sept.	15

TABLE 3
ECHELLE ORDERS

Order	Wavelength Range
1	5285-5340 Å
2	5415-5470 Å
3	5550-5605 Å
4	5690-5750 Å
5	5840-5900 Å
6	6000-6060 Å
7	6165-6230 Å
8	6340-6405 Å
9	6530-6595 Å

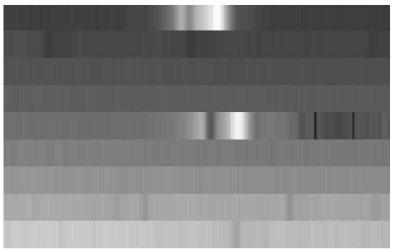

FIG. 1.— This grayscale plot shows the nine levels of stacked data. The Hα line is evident in the top band.

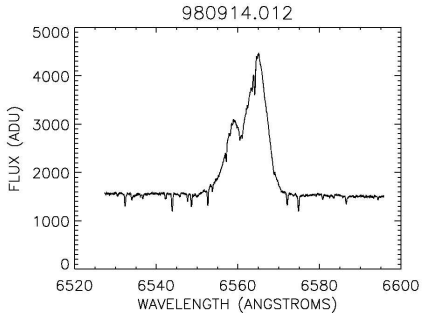

FIG. 2.— This plot shows one example the extracted Hα line spectrum, shown in Analog-to-Digital units (ADU's).

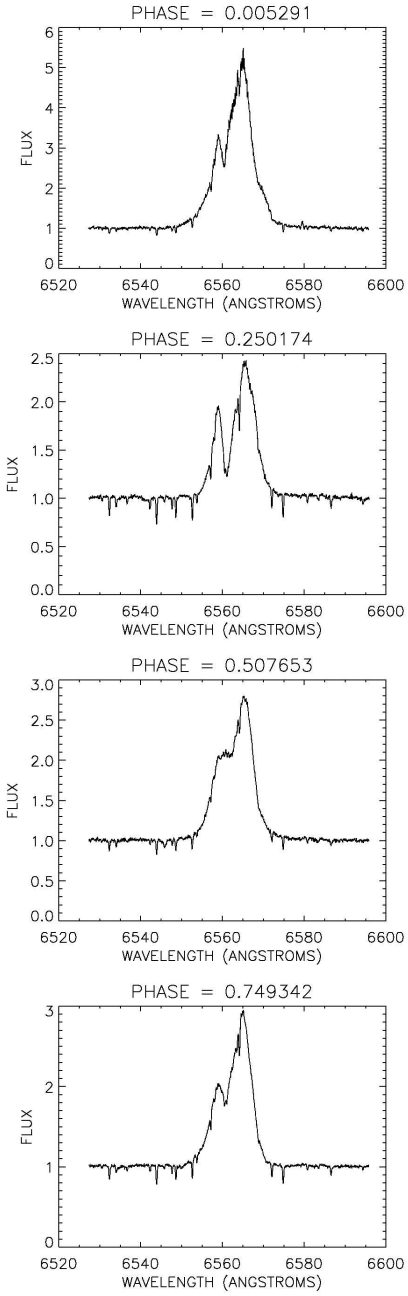

FIG. 3.— These plots show examples of the Hα line profi le at approximately quarter phase intervals as the component stars complete one orbit.

$$EW = \int_{-\infty}^{\infty} \left[\frac{F_\lambda}{F_c(\lambda_\circ)} - 1 \right] d\lambda \,, \tag{2}$$

or

$$EW = \frac{F_l}{F_c}, \tag{3}$$

where F_l represents the total line flux and F_c represents the continuum level of the line at $\lambda_\circ$ = 6562.81 Å. We used the relative light curve of Harmanec et al. (1996) to determine the relative continuum level (see Appendix A).

Plots of the equivalent width (top panel) with phase and the optical light curve (bottom panel) are shown in Figure 4. We find the Hα equivalent width varies with phase. It obtains its largest value during the primary eclipse and also increases

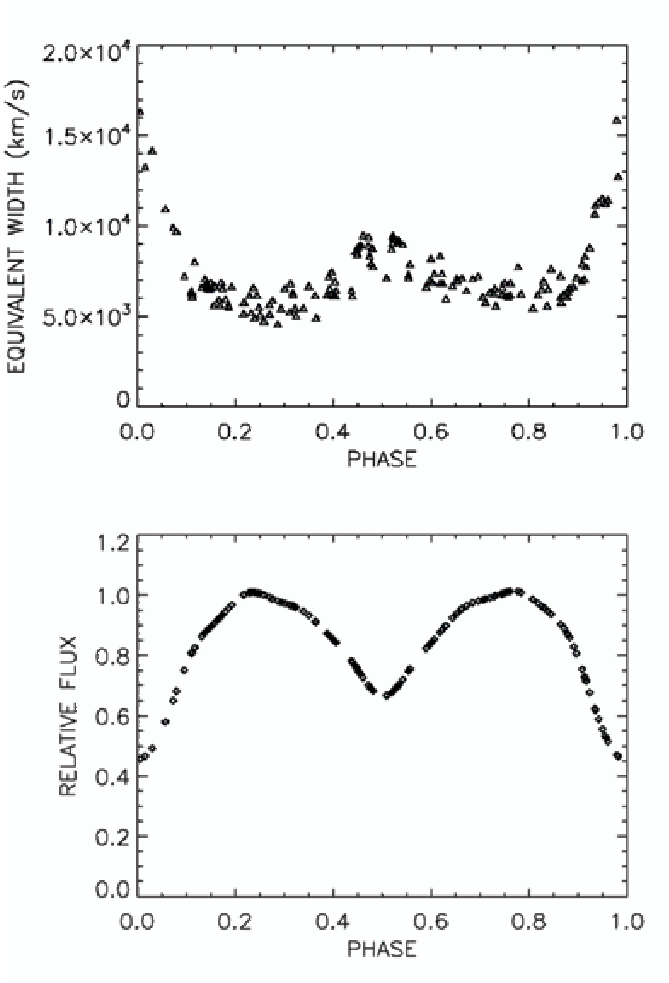

FIG. 4.— The plots of equivalent width and the optical light curve show an inverse relationship.

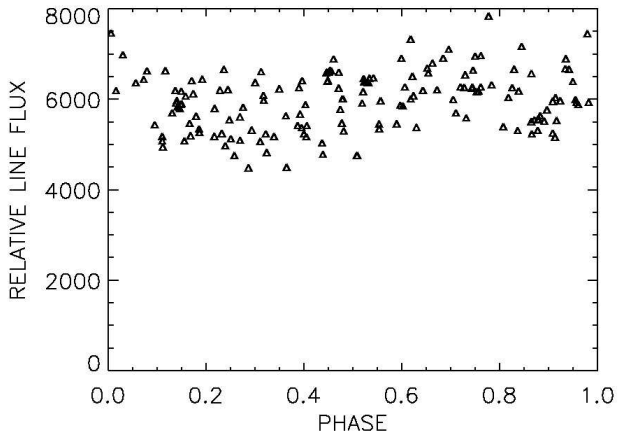

FIG. 5.— This plot shows that although the shape of the Hα emission line profile undergoes drastic changes during the orbital cycle, the total Hα emission does not change with phase.

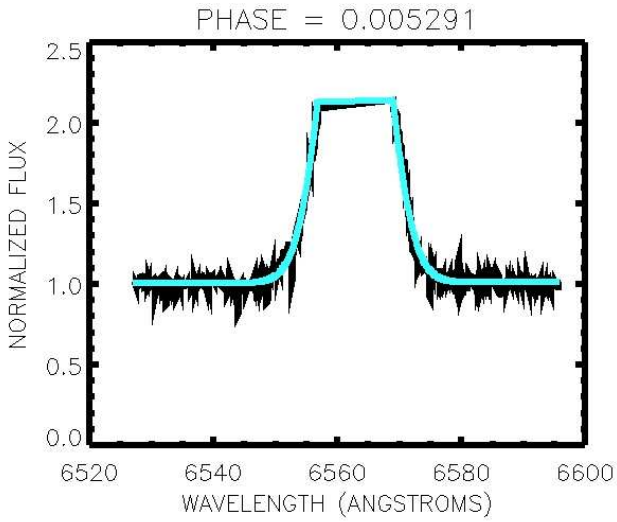

FIG. 6.— This plot shows an Hα emission line profile with the data points between 6557-6569Å removed. The IDL Gaussian procedure was used to fit the wings of the Hα line profile.

somewhat during the secondary eclipse. Comparing the optical light curve, the Hα emission is seen to be cyclical and is distinctly influenced by the two eclipses. We conclude that the equivalent width and the optical light curve are inversely related, and this relationship is confirmed in Figure 5. This figure shows the total Hα line emission derived by multiplying the equivalent width values by the relative light curve in the optical band for the continuum level from Figure 4. Outside the intrinsic noise in the Hα emission, the total line flux does not vary with phase. With such a lack of variation in the total line emission, plus the observed variations in line profile shape, one would expect that the peak of the line profile should be inversely related to the line width.

We wanted to characterize the line profiles in terms of height and width; however, the shape of the Hα line profile is double peaked and distinctly non-Gaussian. Manual measurement could not be accomplished due to the deep dips in the line profile. To overcome this problem, the data files were modified by excluding the data points between 6557 - 6569 Å. Figure 6 shows how Gaussian fits were obtained for the wings of each Hα spectrum. The IDL Gaussian procedure computes the height of the Gaussian (the peak), the center wavelength of the Gaussian, and the FWHM. (See Appendix B for data obtained using this technique.)

The relative height of the peak of the line profile, shift of line center ($\Delta\lambda$), and HWHM are plotted against phase in Figure 7. Although each of these components of the line profile vary with phase, they differ from what would be expected in the circular orbit of eclipsing stars. The peak of the emission line, when plotted against phase (see Figure 7a), shows a rightward displacement suggesting it lags behind the secondary eclipse by ≈0.1 orbital period. The HWHM plotted against phase (see Figure 7c) exhibits a leftward displacement during the secondary eclipse suggesting it precedes the secondary eclipse by ≈0.1 of the orbital period.

We used a Fourier analysis to fit the line shift data set (see Figure 7b). Although one would expect a zero doppler shift during the eclipse, our fit shows the zero doppler shift at ≈0.6 orbital phase suggesting it lags the eclipse by ≈0.1 of the orbital period. We also note that the bulk of the Hα emission is redshifted. This would suggest that either the redshifted jet is larger than the blueshifted one, or that β Lyrae's inclination angle causes the star components to conceal more of the blueward jet's Hα emission.

Figure 7 shows other relevant comparison plots. The line shift is plotted against the line peak data in Figure 7d. This

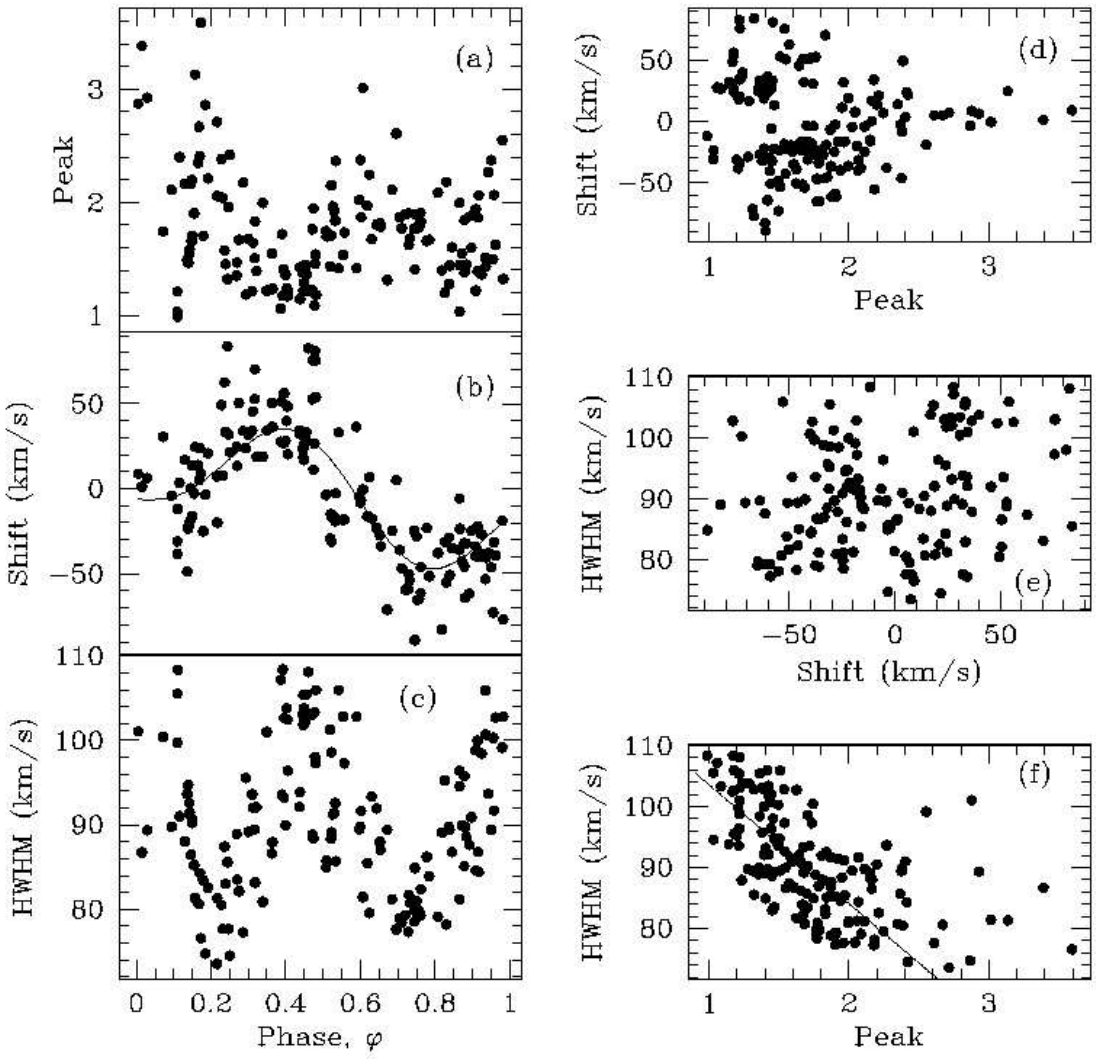

FIG. 7.— The peak, shift, and HWHM are plotted with phase (a,b,c). Other relevant comparison plots are shown (d,e,f) and discussed in the text.

plot shows that when the line profile is tall and narrow, the Hα emission is near zero shift. The HWHM is plotted against the line shift in Figure 7e. There is no correlation between the HWHM and the shift. Plotting the HWHM against the peak results in an inverse linear relationship as predicted (see Figure 7f). When the peak of the line profile is tall, the width is narrow. When the peak of the line profile is short, the emission line is wider such that the total flux does not change with phase. This confirms that the total Hα emission remains constant throughout the orbit and is independent of the location of the component stars.

4. CONCLUSIONS

Using the extracted Hα data, we found that although the Hα emission line profile undergoes drastic changes with phase, the net Hα emission is not seen to vary. Surprisingly, the fact that the two stars eclipse and that the system contains a thick accretion disk appears not to influence the level of Hα emission. Harmanec et al. (1996) and Ak et al. (2007) have claimed that the Hα emission is formed predominantly in the jet-like structures of this system. We agree with their conclusion that the jet-like structures must extend over a substantial volume since the stellar components of β Lyrae have little impact on the total flux of Hα emission.

We are grateful to D. Luttermoser and G. Henson of ETSU and J. Hoffman of the University of Denver for their advice and assistance in completing this project. We thank The Honors College of East Tennessee State University for funding the cost of IDL software and K. Bjorkman of Ritter Observatory for providing the data used in this study. We also thank M. Wood and the SARA REU program for the opportunity to attend the 13th Annual SARA Astrophysical Congress.

APPENDIX

THE LIGHT CURVE OF β LYRAE

We describe the optical light curve observed from β Lyrae with a function Y that depends on phase Φ as given by Harmanec et al. (1996):

$$Y(\Phi) = V + \sum_{j=1}^{7} [A\cos U(\Phi) + B\sin U(\Phi)] \ , \tag{A1}$$

where $Y(\Phi)$ represents the magnitude value at the phase Φ, V = 0.8307974089 is a constant equal to the mean of the light curve, and U, A, and B are coefficients to represent the harmonics in the light curve.

TABLE A1
LIGHT CURVE COEFFICIENTS

j	U	A	B
1	6.2831853072	–0.0700098506	–0.0057556374
2	12.5663706144	–0.2106870444	–0.0059300616
3	18.8495559215	–0.0370618842	0.0007291482
4	25.1327412287	–0.0473236043	–0.0001056881
5	31.4159265359	–0.0058658904	0.0049789641
6	37.6991118431	–0.0126916374	0.0023121238
7	56.5486677646	0.0078856720	0.0000387452

JOURNAL OF Hα DATA

This table contains data that was produced during this project. The spectral line data are listed in phase order. The file names were assigned to each spectrum by observers at the Ritter Observatory. The names represent the date that a spectrum was taken (in Universal Time). The peak, center and FWHM values were obtained using IDL's GAUSSFIT procedure to fit the wings of the Hα line profiles. The occurrence of "N/A" in some rows of the table signify cases where acceptable fits could not be obtained.

FILE NAME	PHASE	PEAK	CENTER (Å)	FWHM (Å)	EW (Å)
19971003.014	0.005291	2.8744868	6563.0021	4.4240228	16339.00
19990712.024	0.015438	3.3878101	6562.8375	3.7965085	13266.00
19980428.032	0.029435	2.9272383	6562.9517	3.9106898	14180.60
19980905.012	0.056088	N/A	N/A	N/A	10967.00
19970731.013	0.072153	1.7420130	6563.4798	4.3966191	9898.66
19970921.014	0.079044	N/A	N/A	N/A	9715.08
19990713.024	0.094867	2.1116500	6562.7196	3.9292614	7235.56
19990916.022	0.109916	1.0306668	6562.1321	4.6197098	6415.99
19990821.029	0.110113	1.2091217	6561.9709	4.3655456	6284.50
19990903.025	0.111204	0.98615616	6562.5495	4.7427306	6102.76
19980703.016	0.116191	2.4015459	6562.8865	3.9837116	8026.34
19980906.012	0.130363	2.1631254	6563.1809	3.8533042	6615.60
19970610.037	0.136694	1.4923599	6561.7425	4.0983204	7087.13
19970706.014	0.138458	1.5042122	6562.2955	4.1454875	6745.32
19970706.016	0.139760	1.4639587	6562.3189	4.1474977	6783.38
19970706.018	0.141638	1.5430141	6562.3308	4.0528368	6607.03
19970706.020	0.143670	1.5866029	6562.3823	4.0057192	6561.82
19970801.016	0.146213	2.1626155	6562.8174	3.7849597	6498.31
19970706.024	0.147853	1.6569294	6562.4374	3.9752386	6580.73
19970814.012	0.149042	2.1975201	6563.1108	3.9610680	6894.83
19970706.026	0.149726	1.7039302	6562.4546	3.9490740	6582.01
20000805.018	0.155084	1.9008458	6562.7500	3.7295801	5609.20
19970922.014	0.157828	3.1319504	6563.3498	3.5597328	6669.70
20000913.014	0.165965	2.3477425	6563.1185	3.5338205	5922.63
19990701.016	0.168061	2.6704991	6562.9215	3.5279377	5609.43
19971031.012	0.170074	2.4113991	6563.3334	3.6900258	6896.17

FILE NAME	PHASE	PEAK	CENTER (Å)	FWHM (Å)	EW (Å)
19990618.020	0.173214	3.5930691	6563.0065	3.3516555	6548.58
19960830.012	0.179073	1.7025485	6562.2620	3.6523220	5951.22
19990809.031	0.185142	2.8632243	6562.7340	3.2717777	5587.30
19990904.022	0.185869	N/A	N/A	N/A	5498.63
19980608.022	0.191947	2.2116427	6563.2678	3.6135373	6660.42
19970720.012	0.216503	2.7140687	6562.9707	3.2191064	5174.58
19970624.014	0.216895	2.0563850	6562.3744	3.5586124	5788.70
19970828.012	0.228099	2.3834720	6563.8891	3.5244014	6147.69
19970720.022	0.231715	2.0413903	6562.9795	3.4004852	5193.95
19971006.012	0.236211	1.5734147	6564.1812	3.8260207	6595.28
20000901.016	0.238867	1.4509456	6563.5384	3.6335177	4924.81
19971019.012	0.244160	1.3211697	6564.6477	3.7451807	6164.72
19990619.016	0.247221	1.9587771	6563.5098	3.3997089	5508.03
19990715.024	0.250174	2.4197103	6563.2825	3.2614342	5099.67
19990728.031	0.257391	N/A	N/A	N/A	4752.15
19980527.017	0.268877	1.3495274	6563.3478	3.8920030	5653.67
19990905.029	0.269061	1.4658193	6563.1021	3.6544871	5129.42
19980705.021	0.275160	1.6687363	6563.9147	3.5949605	5891.76
19980826.014	0.286111	2.1761007	6563.5559	3.3819978	4572.79
19970721.012	0.292954	1.1803138	6563.3331	4.1826235	5448.25
19970803.014	0.300082	1.6773673	6563.5066	3.9031166	6547.01
20000820.012	0.310298	1.2118192	6563.5566	4.0974391	5234.32
19970829.012	0.312023	1.6426180	6563.8057	4.0282854	6834.82
19971007.014	0.316956	1.5055908	6563.9664	3.9152847	6310.39
19971020.012	0.317689	1.8307166	6564.3487	3.6404341	6199.95
20000902.020	0.321461	1.3906506	6563.2188	4.0304473	5444.71
19990716.024	0.323606	N/A	N/A	N/A	5025.40
19990811.029	0.338385	1.9937958	6563.2220	3.5408063	5468.35
19980706.014	0.349337	1.2175910	6563.5611	4.4214508	6681.71
19980909.014	0.362657	1.5467288	6563.9152	3.7910952	6168.43
19980827.012	0.364351	1.2333941	6563.6065	3.8487424	4940.37
20000808.017	0.386794	1.0583646	6563.4164	4.6909758	6199.96
19970925.012	0.389398	1.7189614	6563.9338	4.0968056	7198.71
20000821.020	0.391881	1.1714858	6563.4149	4.7440379	6556.10
20000903.015	0.394745	1.4055701	6563.3982	4.0801766	6241.59
19971021.014	0.395894	1.1753159	6564.0382	4.4917328	7467.83
19990621.024	0.399575	1.3586355	6563.4248	3.9383034	6145.11
20000916.015	0.402765	1.2380938	6563.6820	4.5439396	6942.52
20000929.018	0.404308	1.1678484	6563.8712	4.4840212	6126.10
19990717.024	0.405539	1.2150388	6563.2541	4.2203908	6430.46
19980828.014	0.436638	1.4237519	6563.5570	4.0323470	6432.42
19980802.033	0.438410	1.1416957	6563.5144	4.1079579	6144.36
19970710.014	0.444881	1.3748373	6563.3191	4.5096947	8616.15
19970710.016	0.446922	1.4224954	6563.3431	4.4587429	8705.38
19970627.018	0.447348	1.2132033	6563.2070	4.6131646	8447.47
19970627.019	0.448485	1.2846748	6563.1765	4.5430891	8505.79
19970710.020	0.451161	1.4436791	6563.3983	4.4692183	8824.13
19970710.022	0.453314	1.4222989	6563.4825	4.5272241	8942.58
19970710.024	0.455237	1.3606088	6563.5360	4.6148558	8984.38
19970831.012	0.460048	1.2166294	6564.6185	4.7316085	9490.36
19970913.012	0.470728	1.2214300	6564.4676	4.5109324	8905.73
19971009.012	0.470776	1.7605530	6563.9636	3.8881713	9403.89
19990609.020	0.473930	1.9490266	6563.0579	3.8679865	8315.74
19990622.029	0.476843	1.0849410	6563.3897	4.5226375	7937.59
20000917.018	0.478152	1.4571321	6564.5854	4.2919033	8739.29
20000917.020	0.479681	1.5392268	6564.4629	4.2597957	8778.77
20000930.016	0.480775	1.1780933	6563.9917	4.6383667	7763.86
19980803.015	0.507653	1.7444671	6562.7275	3.7188174	7130.46

FILE NAME	PHASE	PEAK	CENTER (Å)	FWHM (Å)	EW (Å)
19980803.016	0.508669	1.6977407	6562.7371	3.7539618	7135.87
19970520.035	0.518597	1.4323880	6562.1707	4.4328405	8729.37
19970711.014	0.520699	2.1485300	6562.4832	3.8678091	9071.16
19970615.037	0.521637	1.7050568	6562.1286	4.3154436	9470.79
19970711.016	0.522893	2.1515403	6562.4563	3.9015182	9341.97
19970711.018	0.525207	1.9636840	6562.4372	3.9932665	9287.29
19970711.022	0.529684	1.9218847	6562.4469	4.0028038	9164.92
19970711.024	0.532040	1.8367520	6562.3931	4.0519076	9087.09
19970806.012	0.533515	2.3653477	6562.7521	3.7511590	9193.19
19970927.012	0.541409	1.4153750	6563.5370	4.6380111	8984.66
19990706.024	0.553287	1.5353416	6562.4070	4.5015644	7291.53
19971010.014	0.553572	N/A	N/A	N/A	7141.54
19990623.033	0.556191	1.7324889	6562.4121	4.2579948	7903.02
19980830.012	0.589178	1.4172193	6563.6064	4.5002883	6634.10
19970712.012	0.596437	2.0219295	6562.7151	3.9166751	7014.46
19970629.018	0.598879	2.3766300	6562.6307	3.9300261	8206.33
19970712.016	0.601682	1.8655769	6562.6639	4.0129505	6919.97
19970725.015	0.605824	3.0133929	6562.8021	3.5646202	7346.42
19970902.014	0.617834	N/A	N/A	N/A	8360.16
20000811.016	0.617851	1.9702483	6562.4557	3.7409365	6849.94
19970928.012	0.621436	N/A	N/A	N/A	7362.37
19971011.012	0.623511	2.2447908	6562.9599	3.4816498	6845.28
19990707.024	0.629559	1.6739355	6562.4269	4.0861177	5979.89
19990802.031	0.642811	1.8026774	6562.3055	4.0244469	6700.13
19990923.013	0.651883	1.8136627	6562.2115	3.8502070	7115.60
19980519.030	0.653602	1.7818969	6562.0725	3.8090741	6977.50
19980710.038	0.662296	N/A	N/A	N/A	7121.77
19970522.039	0.671628	1.3115295	6561.2522	3.9149992	6431.77
19970808.015	0.684196	2.1109436	6562.2693	3.5541849	7083.84
19970916.014	0.695388	2.6083922	6562.9201	3.3974754	7240.68
20000825.020	0.704849	1.8685607	6562.0192	3.4535346	6085.56
19990708.026	0.710134	1.7709489	6561.7876	3.4314317	5776.70
19990803.031	0.719314	1.8965208	6561.5091	3.4713351	6328.39
19990816.029	0.727211	1.9016115	6561.5142	3.3844149	6291.43
19990924.014	0.729276	1.6225598	6561.7075	3.5758919	6566.96
19990829.029	0.731141	1.6819145	6561.6291	3.5338521	5599.03
19980901.014	0.743317	1.7674263	6562.2673	3.5003941	6217.39
19980901.015	0.743999	1.8951391	6562.2732	3.4379810	6241.13
19970605.020	0.745219	1.4029089	6560.8584	3.7160061	6600.67
19980914.012	0.749342	1.7753451	6562.1973	3.5424648	6893.87
19970714.012	0.752554	1.7697995	6561.3805	3.4608374	6108.62
19970714.016	0.756800	1.7873515	6561.3862	3.4920589	6104.08
19970714.020	0.760999	1.9086233	6561.4690	3.4707083	6189.67
19970809.013	0.761226	1.8311594	6561.7973	3.6063240	6876.20
19970904.016	0.777030	1.6567044	6562.3021	3.7743840	7744.67
19990626.026	0.783443	1.6660568	6561.6829	3.6726160	6260.99
19990830.031	0.807163	2.0849916	6561.9809	3.4630942	5468.22
19970511.016	0.817578	1.3984760	6560.9982	3.8991868	6200.82
19980902.016	0.825225	1.1977781	6562.1256	4.1701705	6492.20
19970702.016	0.829278	2.1805166	6561.6011	3.4220513	6957.82
19981024.014	0.836386	1.2763005	6562.1791	3.9276567	5594.92
19970810.012	0.838499	1.4389695	6561.6956	3.9124543	6533.48
19970905.014	0.844569	1.6030602	6562.0422	3.7977447	7642.78
19960813.009	0.864391	1.9957821	6562.0180	3.5535673	6084.27
19971109.014	0.864502	1.4438629	6562.6840	4.2193553	7264.00
19990723.024	0.865315	1.0320392	6562.2939	4.1396640	5791.54
19990710.024	0.870579	1.5463339	6561.8761	3.9369620	6219.40
19990818.029	0.877419	1.8419402	6561.8108	3.7249635	6354.48
19990831.024	0.877523	1.3789534	6562.1094	4.1906558	6080.59
19980522.024	0.879320	1.4168074	6561.4053	3.9278453	6404.59

FILE NAME	PHASE	PEAK	CENTER (Å)	FWHM (Å)	EW (Å)
19990926.022	0.882395	1.4485416	6562.1046	3.8776604	6569.01
19970429.025	0.890754	1.8747881	6561.4600	3.8363212	6652.46
19980821.014	0.896255	1.5958657	6562.2642	3.9791689	7142.27
19980929.025	0.907966	1.2163886	6562.0660	4.3258292	6962.05
19970703.012	0.908170	1.9378816	6561.9427	3.7042903	7904.41
19981012.017	0.912885	1.3916459	6562.3274	4.3758654	7068.59
19970703.018	0.913920	1.8670915	6561.9979	3.7995569	8322.92
19970716.032	0.915938	2.0646738	6561.9336	3.6936801	7736.08
19970919.012	0.923347	1.3601599	6562.2226	4.3094840	8808.86
19990615.016	0.933758	1.5066739	6561.6423	4.6361512	10687.80
19971015.014	0.934850	1.4328822	6561.9243	4.4073417	11138.60
19990711.024	0.941315	2.2685795	6561.9842	4.1001977	11312.30
19990806.016	0.949272	2.3746640	6561.7976	3.9134539	11527.80
19980427.024	0.954796	1.4945551	6561.2161	4.3906539	11242.10
19990914.012	0.956813	2.0654718	6562.1218	4.0129143	11275.60
19990901.029	0.960347	1.6239432	6561.9519	4.4957604	11437.50
19980727.033	0.978918	2.5507375	6562.3964	4.3405383	15860.00
19970513.032	0.981534	1.3196904	6561.1251	4.5004695	12733.50

REFERENCES

Ak, H. et al., 2007, A&A, 463, 233
DeGreve, J. P., & Linnell, A. P. 1994, A&A, 291, 786
Harmanec, P. et al., 1996, A&A, 312, 87
Harmanec, P., & Scholz, G. 1993, A&A, 279, 131
Hoffman, J. L., Nordseick, K. H., & Fox, G. K. 1998, AJ, 115, 1576
Linnell, A. P., Hubeny, I., & Harmanec, P. 1998, ApJ, 509, 379